A Minimal Gating Model for the Cardiac Calcium Release Channel

Alexandra Zahradníková and Ivan Zahradník
Institute of Molecular Physiology and Genetics, Slovak Academy of Sciences, 833 34 Bratislava, Slovak Republic

ABSTRACT A Markovian model of the cardiac Ca release channel, based on experimental single-channel gating data, was constructed to understand the transient nature of Ca release. The rate constants for a minimal gating scheme with one Ca-free resting state, and with two open and three closed states with one bound Ca^{2+}, were optimized to simulate the following experimental findings. In steady state the channel displays three modes of activity: inactivated I mode without openings, low-activity L mode with single openings, and high-activity H mode with bursts of openings. At the onset of a Ca^{2+} step, the channel first activates in H mode and then slowly relaxes to a mixture of all three modes, the distribution of which depends on the new Ca^{2+}. The corresponding ensemble current shows rapid activation, which is followed by a slow partial inactivation. The transient reactivation of the channel (increment detection) in response to successive additions of Ca^{2+} is then explained by the model as a gradual recruitment of channels from the extant pool of channels in the resting state. For channels in a living cell, the model predicts a high level of peak activation, a high extent of inactivation, and rapid deactivation, which could underlie the observed characteristics of the elementary release events (calcium sparks).

INTRODUCTION

The mechanism of calcium gating of the calcium release channel (ryanodine receptor type) of both cardiac and skeletal muscle sarcoplasmic reticulum subtypes has been the subject of extensive experimental studies (for a review, see Coronado et al., 1994). Paradoxically, after reconstitution into planar lipid membranes, the two subtypes are activated by calcium in a very similar way (Chu et al., 1993; Györke et al., 1994), in spite of the fact that under physiological conditions only the cardiac type requires calcium to trigger release (Rios and Brum, 1987; Fabiato, 1985). Another paradox concerns their inactivation mechanism, which was found to be calcium dependent for the skeletal type, but calcium independent for the cardiac type (Smith et al., 1988; Chu et al., 1993), despite the fact that upon activation under physiological circumstances both are expected to be exposed to an explosive increase in the Ca^{2+} concentration in their vicinity (Escobar et al., 1994; Cannell et al., 1994, 1995; López-López et al., 1995; Klein et al., 1996; Shacklock et al., 1995; Tsugorka et al., 1995). The calcium-dependent mechanism of inactivation can easily be envisioned as a transition of the activated channel to a closed (inactivated) state upon binding of another Ca^{2+} ion. It is not obvious, however, how the inactivation works without binding of Ca^{2+}, as might be the case for the cardiac RyR subtype.

It is known that activation of the calcium release channel (CRC) by calcium ions induces two distinct bursting patterns of activity (Ashley and Williams, 1990; Sitsapesan and Williams, 1994), brought about by slow processes that have been experimentally characterized as three distinct modes of channel gating (Zahradníková and Zahradník, 1995a). The presence of gating modes with very different open probabilities may have important implications for the dynamics of channel gating during large and abrupt concentration changes of cytoplasmic Ca^{2+}, taking place during the excitation-contraction-relaxation cycle of a cardiac cell. In bilayer experiments with cardiac CRC, abrupt changes in Ca^{2+} using caged calcium and a laser pulse to generate a step increase in free Ca^{2+} in the vicinity of CRC (Györke and Fill, 1993) induce a transient increase in channel activity. The underlying molecular mechanism of this rather complex process, termed "adaptation," has not yet been elucidated at the single-channel level, although several models reproducing some features of ensemble open probability have recently been reported. These models, however, predict either a calcium-dependent inactivation of steady-state P_o (Tang and Othmer, 1994) or a prolongation of channel open times with increasing Ca^{2+} (Cheng et al., 1995; Sachs et al., 1995), features that are not observed in single-channel measurements.

In this paper, using modeling and simulation, we test the hypothesis that the process of the cardiac Ca release channel adaptation arises from time-dependent transitions of the channel between individual modes of gating. We introduce the concept of fast-access and slow-access states, which makes testing of the dynamic channel behavior possible. We constructed the simplest possible model, based on experimental data where the channel was activated by Ca^{2+} in the absence of other physiological modulators such as ATP or Mg^{2+}. This model simulates the steady-state behavior of CRC at the single-channel level, i.e., its open and closed lifetimes, bursting patterns, and modal gating, and at the macroscopic level, i.e., its rate of activation and inactivation. We also show some predictions of the model that can be experimentally verified.

Received for publication 18 December 1995 and in final form 18 September 1996.

Address reprint requests to Dr. Alexandra Zahradníková, Institute of Molecular Physiology and Genetics, Slovak Academy of Sciences, Vlárska 5, 833 34 Bratislava, Slovak Republic.

0006-3495/96/12/2996/17 $2.00

MATERIALS AND METHODS

The Mathematica program (version 2.2; Wolfram Research) implemented on an AT 486 machine was used for modeling. Channel kinetics was described by a matrix of transition rates between individual channel states of the analyzed gating schemes (Colquhoun and Hawkes, 1982, 1983). Steady-state probabilities of individual open and closed states were obtained by solving the system of equilibrium equations, describing the equilibria between channel states as ratios of transition rates. Theoretical probability density functions of open and closed time distributions were computed according to the method of Colquhoun and Hawkes (1982).

The time course of the probabilities P_i of the individual states after application of a step change in *cis* calcium concentration was calculated by solving a system of ordinary differential equations of channel kinetics (Eq. 1):

$$\frac{dP_i}{dt} = -P_i \sum_{i,i\neq j} k_{ij} + \sum_{j,j\neq i} (k_{ij}P_j), \quad (1)$$

where P_i's (P_j's) are the probabilities of state $i \neq j$ ($j \neq i$), and k_{ij} are the transition rate constants from state i to state j. Initial conditions were obtained either from the solution of equilibrium equations, if the step change was applied from the steady state, or fed in from a previous solution of differential equations if the step occurred at a time before reaching steady state. We will refer to the kinetics of channel activation computed in this way as theoretical kinetics.

The apparent calcium sensitivity of open probability P_o, probability of mode occurrence P_M, and within-mode open probability $P_{o,M}$ were described by the general equation (Eq. 2), to which we will refer as theoretical calcium dependence:

$$P_{\mathscr{X}} = \frac{\sum_{i\notin\mathscr{X}} K_i[\mathrm{Ca}]}{\sum_{j\in\mathscr{X}^{\sim\mathscr{S}}} K_j[\mathrm{Ca}] + \sum_{i\in\mathscr{X}} K_i[Ca] + 1} = P_{max}\frac{[\mathrm{Ca}]}{K_{Ca} + [\mathrm{Ca}]}, \quad (2)$$

where

$$P_{max} = \frac{\sum_{i\in\mathscr{X}} K_i}{\sum_{j\in\mathscr{X}^{\sim\mathscr{S}}} K_j + \sum_{i\in\mathscr{X}} K_i},$$

and

$$K_{Ca} = \frac{1}{\sum_{j\in\mathscr{X}^{\sim\mathscr{S}}} K_j + \sum_{i\in\mathscr{X}} K_i}.$$

K_i (or K_j) is the equilibrium constant of the ith (or jth) state relative to the resting state R, $\mathscr{X}$ stands for the examined set of states (e.g., open states, fast-access states, etc.), $\mathscr{S}$ is the set of all participating states, and $\mathscr{X}^{\sim\mathscr{S}}$ is the complement of $\mathscr{X}$ in $\mathscr{S}$.

The calcium dependence of P_o, P_M, and $P_{o,M}$ for simulated data was obtained by fitting the evaluated probabilities with Eq. 3:

$$P = P_{max}\frac{[\mathrm{Ca}]}{K_{Ca}^{app} + [\mathrm{Ca}]}. \quad (3)$$

The extent of inactivation was expressed as $h_\infty = (P_{o,peak} - P_{o,steady})/P_{o,peak}$.

Stretches of single-channel activity were simulated with the CSIM program (Axon Instruments), using an AT 486 computer, and analyzed with TRANSIT software (Baylor College of Medicine, Houston, TX) as in Zahradníková and Zahradník (1995a). In the simulated records, the rms of the background noise after filtering at 2 kHz was set to 12.5% of the single-channel amplitude. To resolve all closed time components, stretches of data containing at least 10,000 openings had to be simulated, which in the case of 0.1 and 0.5 μM Ca^{2+} amounted to 2000-s simulations. The minimum duration of simulated data was 60 s. The noncumulative histograms of open and closed times were fitted by sums of exponentials using the minimum χ^2 method, and all other secondary analyses, calculations, statistics, and graphics were done using Origin version 3.50 (Microcal Software, Northampton, MA). It should be noted that the theoretical parameters, obtained from Eqs. 1 and 2, provide a full description of the model. In contrast, the parameters of the model obtained by analysis of simulated data are subjected to limitations similar to those of the experimental data, i.e., to finite sampling frequency and effects of noise and filtering, resulting mostly in missing very fast events.

CONSTRUCTION OF THE MODEL

Identification of modes and states

The basic framework of our model was built on four experimental observations with the CRC reconstructed into lipid bilayers. First, analysis of steady-state activity of the cardiac CRC activated by calcium established a minimum of two open ($\tau_{o1} < \tau_{o2}$) and three closed ($\tau_{c1} < \tau_{c2} < \tau_{c3}$) lifetimes (Ashley and Williams, 1990; Chu et al., 1993; Zahradníková and Zahradník, 1995a). Second, changes in channel activity on a slow time scale were shown to result from transitions between modes with time constants of about 1 s (Zahradníková and Zahradník, 1995a). Three mode types (the open modes L and H, and the closed inactivated mode I) displayed two types of transitions among them, meaning that modes are arranged in series. Third, burst analysis within modes revealed that each of the two open modes most probably contains one closed and one open state (Zahradníková and Zahradník, 1995a). Fourth, when challenged with a step increase in Ca^{2+} concentration, the CRC responds with a transient increase in activity (Györke and Fill, 1993).

It was hypothesized (Zahradníková and Zahradník, 1995a) that the transient response of CRC activity to a step increase in Ca^{2+} concentration, as reported by Györke and Fill (1993), results from transitions among modes. According to this hypothesis the sharp increase in ensemble channel current in response to a Ca^{2+} concentration pulse can be explained by activation of the channel within the high open probability mode H, because single CRC channels display bursts of high P_o typical for mode H at the commencement of a Ca step, as seen in experiments of Györke and Fill (1993). The subsequent decay of CRC gating activity to the much lower steady-state level proceeds monoexponentially on a seconds time scale (Györke and Fill, 1993), which can be envisioned as an equilibration of the channel into a mixture of modes H, L, and I. This is schematically shown in the top part of Fig. 1. Here the basic idea of a kinetically driven transient behavior of the channel is illustrated: The binding of agonist, in this case the Ca^{2+} ion, is hypothesized to occur only when the channel is in a specific mode of activity—H-mode in our specific case. Furthermore, both binding and unbinding of the agonist are very rapid, so that

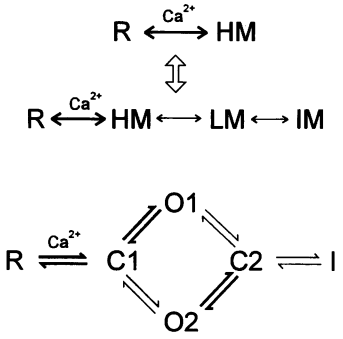

FIGURE 1 The gating scheme of the calcium release channel. (*Upper scheme*) Sequence of intermodal transitions after binding of Ca^{2+} generally expected to produce transient activity of the channel. Early after the Ca^{2+} concentration step, transitions between fast-access states (RHM) prevail. At later times, as indicated by the hollow arrow, the channel equilibrates into the steady-state mixture of all modes. R, resting state; HM, high open probability mode; LM, low open probability mode; IM, inactivated mode. Full double arrows denote fast transitions; light double arrows denote slow transitions. (*Lower scheme*) The state scheme of the calcium release channel minimal model. R, resting state; C1, C2, closed states; O1, O2, open states; I, inactivated (long-lived closed) state. Thin arrows represent slow transitions. Values of the rate constants used for modeling are given in Table 1.

the channel in the agonist-free state R can be considered to still reside in H mode. In the agonist-bound form, the channel can interconvert to the other two modes of activity.

The simplest gating scheme that reproduces the above features, and at the same time is in accord with the results of autocorrelation analysis (Ashley and Williams, 1990; Sitsapesan and Williams, 1994), is shown in the bottom part of Fig. 1. A similar six-state scheme was proposed by Zahradníková and Palade (1993) to explain the inhibitory effects of procaine. These schemes are an extension of a minimal gating scheme of two alternating closed and open states in a loop, connected to the resting state, as suggested by Ashley and Williams (1990). Considering that two of four C ↔ O transitions facing each other in the loop of the gating scheme (*thin arrows* in Fig. 1) have to be in the range of seconds to simulate slow channel gating (Zahradníková and Palade, 1993), it is reasonable to assume that they are involved in intermodal transitions (Zahradníková and Zahradník, 1995a,b). Intramodal analysis revealed that each of the modes L and H contains one distinct open state and at least one distinct closed state. In terms of the gating scheme of Fig. 1 it thus means that states C1 and O1 contribute to mode H activity (high open probability), and states C2 and O2 to mode L activity (low open probability). The remaining long-lived closed state would then correspond to mode I and is annotated in Fig. 1 as I to emphasize its functional correspondence to an inactivated state.

Once we identified modes and states of the scheme, our next step was its quantification. First we assigned functional states, identified by open and closed lifetimes from the steady-state measurements, to states in the gating scheme. Next we estimated the rate constants of transitions between states by solving the equilibrium equations of the scheme, taking advantage of the specific properties of the channel as outlined below. Finally, we tuned the complete system by adjusting the rate constants to approximate all of the available, albeit incomplete, experimental data.

Estimation of rate constants

The slow transitions between open modes, assigned in our scheme to transitions O1 ↔ C2, O2 ↔ C1, make a negligible contribution to the lifetime of either open state. In the framework of our model it means that either of the measured mean open times can be identified with just one (fast) rate constant. Then, taking into account the results of intramodal analysis (Zahradníková and Zahradník, 1995a) that mode H is dominated by long, while mode L by short openings, we can write $k_{O1C1} = 1/\tau_{o2}$ and $k_{O2C2} = 1/\tau_{o1}$. The rate of I → C2 transition, which represents the exit rate from the inactivated mode I, may be identified in a first approximation with the slowest closed time: $k_{IC2} = 1/\tau_{mI}$.

Insight into very fast events of Ca^{2+} binding to the resting state came from experiments with calcium steps. If activation has to proceed with a time constant of 1–3 ms at $[Ca^{2+}] \leq K_{Ca}$, as observed by Györke and Fill (1993) and Györke et al. (1994), then the state C1 has to be short-lived and, moreover, the rate constant k_{C1O1} has to be very large and much larger than the slow k_{C1O2}. Otherwise the activation rate would be slow, and short isolated openings would be observed at the onset of Ca pulses. These criteria are matched only by τ_{c1}, the shortest of the observed closed times. The analysis of channel lifetimes during transitions within mode L and burst analysis (Zahradníková and Zahradník, 1995a) supports the connection of C1 with the open state of longer lifetime, approximated by τ_{o2}, which provides the CRC with bursts and mode H. The exact value of τ_{c1} is not known, as the experimentally measured values were shown to be frequency limited (Sitsapesan and Williams, 1994; Zahradníková and Zahradník, 1995a). Consequently, the corresponding rate constants k_{C1O1} and k_{C1R} (neglecting the very slow k_{C1O2}) cannot be determined directly. The remaining medium closed time can be assigned to the only remaining closed state C2. In addition, as k_{C2O1} was already identified to be very slow, k_{C2O2} should be almost equal to $1/\tau_{c2}$. The correspondence between C2 and τ_{c2}, and their connection to O2 (τ_{o1}), are also in agreement with the results of the burst analysis (Ashley and Williams, 1990; Sitsapesan and Williams, 1994; Zahradníková and Zahradník, 1995a). The respective numerical values used in the model, $1/\tau_{o1} = k_{O2C2} = 3000\ s^{-1}$, $1/\tau_{o2} = k_{O1C1} = 500\ s^{-1}$, $1/\tau_{c2} = k_{C2O2} = 100\ s^{-1}$, $1/\tau_{mI} = k_{IC2} = 1.5\ s^{-1}$, are based on published data (Chu et al., 1993; Sitsapesan and Williams, 1994; Zahradníková and Zahradník, 1995a).

The next step was to assign a rate constant to the transition R → C1. The value used previously (Zahradníková and Palade, 1993), based on the comparison of the Ca binding step with that of the Ca^{2+}-activated potassium channel of

skeletal muscle ($k_{RC1} \sim 10^7$ mol^{-1} s^{-1}), provided transients with very slow activation. The results of Györke and Fill (1993) dictated an increase in this rate constant, to accomplish an activation of the channel by 1 μM Ca^{2+} within 1–3 ms. This was obtained by setting k_{RC1} to 10^9 mol^{-1} s^{-1}, a value that is comparable to the association rate constants of Ca^{2+} with fast fluorescent dyes (Eberhard and Erne, 1989) and can be considered as an upper estimate.

The considerations outlined above enabled the estimation of five out of 12 rate constants. The remaining seven slow constants were found by solving the model's equilibrium equations for the peak and for the steady state in parallel. In our case the peak can be approximated by a quasi-equilibrium of the resting state R with the fast-access H-mode states C1 and O1, because these are reached about 3 orders of magnitude faster than the full equilibrium (compare rates of activation and inactivation in Györke and Fill, 1993). This helps to avoid differential equations, as we could express the peak open probability $p_{o,p}$ as $p_{O1,H}$ (probability of O1 in mode H). The steady-state open probability was found from the complete set of equilibrium equations. The rate constants were then determined by using simple relations as input conditions. First, the relation $k_{C1O1} \times k_{O1C2} \times k_{C2O2} \times k_{O2C1} = k_{C1O2} \times k_{O2C2} \times k_{C2O1} \times k_{O1C1}$ must hold, because of the principle of microscopic reversibility. Second, five criteria that should be met to reproduce the experimentally observed channel characteristics at both the peak and the steady state have been selected from available experimental data at characteristic Ca^{2+} concentrations: 1) At $[Ca^{2+}]$ much larger than K_{Ca}, at which the probability of entering the resting state approaches zero, the maximum open probability at the peak $P_{o,p} = P_{O1,H}$ should approach 1 (we have seeded $P_{O1,H} \sim 0.95$, according to the data of Györke and Fill, 1993); 2) In steady state, P_o should be equal to the maximum steady-state open probability $P_{o,s} = P_{O1} + P_{O2} = P_{O1,H}P_H + P_{O2,L}P_L$ (we have seeded $P_{o,s}$ to ~0.2, in accordance with several published reports: Ashley and Williams, 1990; Sitsapesan and Williams, 1994; Zahradníková and Zahradník, 1995a); 3) The steady-state probability of the inactivated state should correspond to the occurrence of I mode, P_I (the value of P_I we have estimated to be ~0.2; Zahradníková and Zahradník, 1995a); 4) The activation should produce a measurable transient, i.e., $P_{o,p}$ should be larger than $P_{o,s}$ for $[Ca^{2+}] \geq K_{Ca}/x$ ($x > 4$, according to Györke and Fill, 1993); 5) Half-activation of the channel in steady state is in the micromolar range (Chu et al., 1993; Györke and Fill, 1993). Of these five criteria, only four are independent. Thus for certain sets of input values the system has no solution. Furthermore, for low input values of k_{C1O1}, some of the computed rate constants were negative. With the seeded values of $k_{C1R} = 100{,}000$ s^{-1}, $k_{C1O1} = 10{,}000$ s^{-1}, $k_{C2I} = 0.5$ s^{-1}, and the relationships of $k_{C1O2}/k_{O2C1} = 2$ and $k_{O1C2}/k_{C2O1} = 3$, the solution gave values of $P_{O1,H} = 0.952$, $P_{O,s} = 0.214$, $P_I = 0.194$, $K_{Ca} = 0.971$ μM, and $x = 7.76$ (which means that the activation of the channel becomes transient at steps to $[Ca^{2+}] \geq 0.971/7.76 = 0.13$ μM). Finally, for the values of the slow transitions, (i) k_{O1C2} will determine the rates of both inactivation and exit from mode H (because $P_{O1} \gg P_{C1}$), (ii) k_{O2C1} and k_{C2O1} together with k_{C2I} will determine the rate of exit from mode L. By trial and error, we obtained the values of $k_{O2C1} = 0.5$ s^{-1} and $k_{O1C2} = 2.0$ s^{-1}. Thus all slow rate constants in the model (k_{C1O2}, k_{O1C2}, k_{O2C1}, k_{C2O1}, k_{IC2}, and k_{C2I}) are in the range of 0.5–2 s^{-1}. These values are close to the measured intermodal transition rates (Zahradníková and Zahradník, 1995a) and provide simulations that approximate real experimental data.

The resulting set of rate constants, summarized in Table 1, must be taken as approximate and relative, because of the lack of experimental data regarding certain properties of the channel, such as calcium dependence of modal behavior, and broad-range calcium dependence of the single channel during rapid Ca^{2+} changes. The very good agreement of this simple model with the available experimental data made it possible to take a theoretical approach and inspect the behavior of the virtual CRC under conditions that are not yet experimentally feasible but are of physiological importance. (It should be noted that the gating activity was simulated without adjustment to changes in single-channel conductance of the channel at high Ca^{2+}.)

STEADY-STATE ACTIVITY OF THE MODEL AND ITS Ca^{2+} DEPENDENCE

Ca^{2+} dependence of lifetime parameters

Single-channel currents shown in Fig. 2 *A* are representative samples of simulations that demonstrate typical patterns generated by the model upon activation at Ca^{2+} concentrations over 5 orders of magnitude. The simulated currents, which most closely resemble the experimental data, are characterized by their random spiking activity at low $[Ca^{2+}]$ (below 0.5 μM), in contrast to evident modal behavior at higher $[Ca^{2+}]$ (above 1 μM), where bursts with high open probability are interspersed with long closed periods and periods of random openings. As shown, long closures become the more distinct, the higher the activating $[Ca^{2+}]$ that is used.

Kinetic analysis of these simulations confirmed, as expected, the existence of two mean open times and predicted

TABLE 1 Kinetic parameters of the model (Figure 1) used for simulation of channel behavior

k_{RC1} =	$1.0 \times 10^3 \times [Ca^{2+}]$, μmol$^{-1} \cdot$ s^{-1}
k_{C1R} =	1.0×10^5, s^{-1}
k_{C1O1} =	1.0×10^4, s^{-1}
k_{O1C1} =	5.0×10^2, s^{-1}
k_{C1O2} =	1.0×10^0, s^{-1}
k_{O2C1} =	5.0×10^{-1}, s^{-1}
k_{O1C2} =	2.0×10^0, s^{-1}
k_{C2O1} =	6.666×10^{-1}, s^{-1}
k_{O2C2} =	3.0×10^3, s^{-1}
k_{C2O2} =	1.0×10^2, s^{-1}
k_{C2I} =	5.0×10^{-1}, s^{-1}
k_{IC2} =	1.5×10^0, s^{-1}

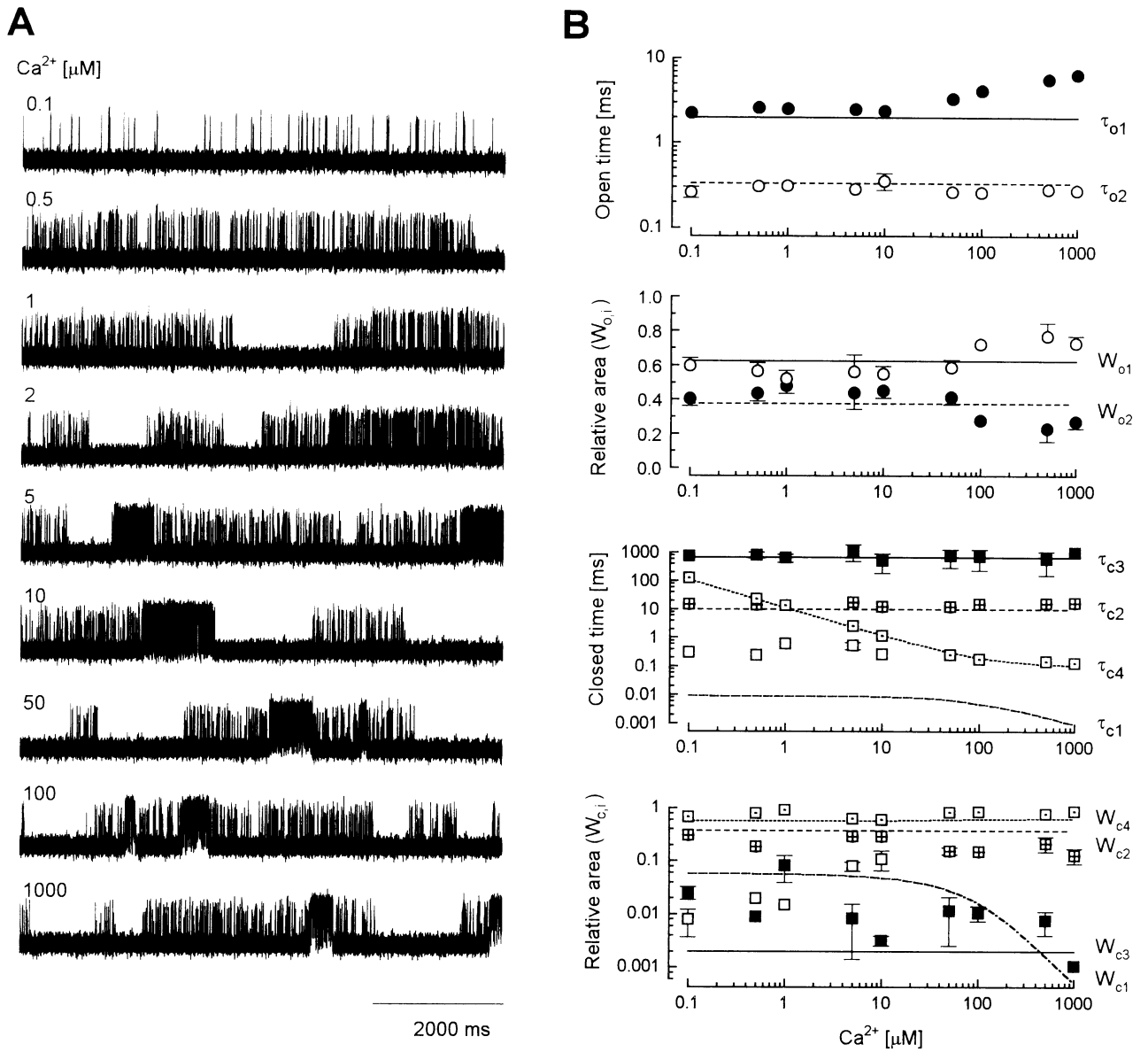

FIGURE 2 Calcium dependence of the simulated Ca release channel activity in the steady state. (*A*) Examples of simulated single-channel traces at different activating Ca^{2+} concentrations (indicated at the left and above the records). (*B*) Lifetime parameters of the model at different Ca^{2+} concentrations. Lines represent theoretical predictions calculated directly from the set of rate constants. Points are the values estimated from simulated traces. *Upper two panels*: Open times. Open circles and dashed lines are for τ_{o1}, and full circles and full lines for τ_{o2}. *Lower two panels*: Closed times. Open, dotted, crossed and full squares, and dashed-dotted, dotted, dashed, and full lines are for τ_{c1}, τ_{c2}, τ_{c3}, and τ_{c4}, respectively. At some Ca^{2+} concentrations, only three closed time components could be detected because of identical values of two lifetimes.

their proportion and lifetime to be independent of $[Ca^{2+}]$ (Fig. 2 *B*). Deviations of the estimated open times (*points*) from the predicted values (*lines*) calculated directly from rate constants arise from the missed closures that are shorter than 200 μs. For high Ca^{2+} the distributions of open times were best fit with three time constants (one of which, in the range of 10–20 ms, was purely artifactual; data not shown). From an experimental point of view it is worth mentioning that this effect increases in its significance at Ca^{2+} concentrations that are two or more orders of magnitude higher than K_{Ca}. The results of this section indicate the extent by which the estimate of the relative contribution of a channel state deviates from the true value, if the lifetime drops below the resolution limit.

Analysis of closed times provided a more complex picture (Fig. 2 *B*). One of the three Ca-independent time constants (*squares*) was found to be close to or below the resolution limit at all Ca^{2+} concentrations. The time constant τ_{c4} decreased with Ca^{2+} concentration and spanned the range from 100 ms to below the time resolution limit. The relative proportions (W_{ci}) of the closed lifetime components did not strongly depend on Ca^{2+} concentration in the range 0.1–100 μM Ca^{2+}. However, the lifetime of the calcium-dependent component (τ_{c4}) was close to τ_{c2} at 0.1

μM Ca^{2+}, and coincided with τ_{c3} around 1 μM Ca^{2+} and with τ_{c1} above 10 μM Ca^{2+}. Therefore it apparently decreased the proportion of long closed time components and increased the short open time components with increasing Ca^{2+}, which resembled the experimentally observed tendencies (Ashley and Williams, 1990; Zahradníková and Zahradník, 1995a).

Ca^{2+} dependence of P_o and modes

The calcium dependence of the steady-state open probability of the simulated traces (Fig. 3 *A*, *open triangles*) was similar to that calculated directly from the rate constants using Eq. 2 (Fig. 3 *A*, *dotted line*). There was a large dispersion in P_o values of individual simulations, which resembled in this respect the experimental data and resulted in a relatively large error in the estimated K_{Ca} (see also Table 2).

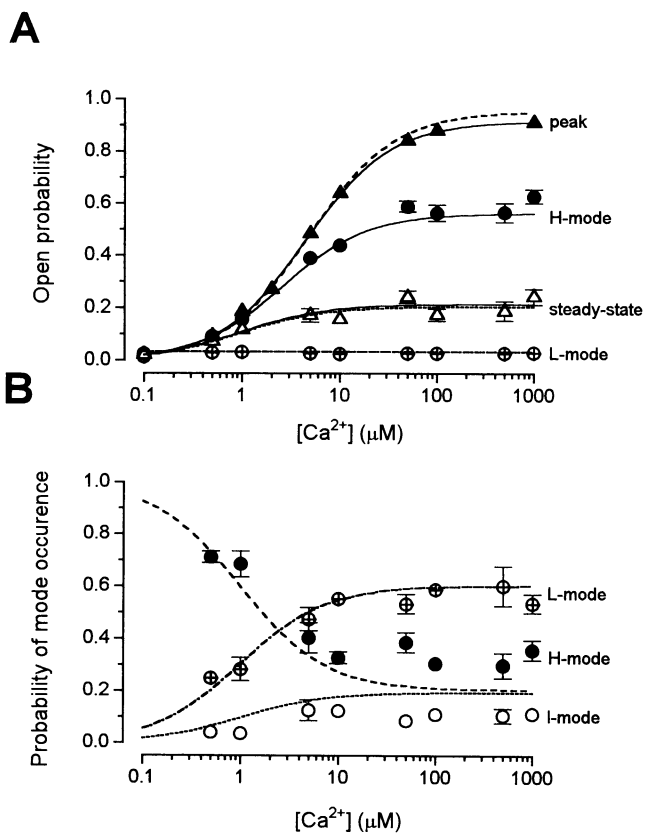

FIGURE 3 Calcium dependence of the characteristic probabilities of the model. (*A*) Calcium dependence of the channel open probability, obtained from analysis of the simulated data in the steady state (△) and at the peak of the transient (▲), and of the within-mode open probabilities for the two open modes (⊕ and ● for modes L and H, respectively). The full lines are the respective hyperbolic fits (with Eq. 3) for the peak open probability, steady-state open probability, and the open probability within H mode. The corresponding theoretical calcium dependencies calculated using Eq. 2 are shown as dashed, dashed-dotted, and dotted lines for H mode, L mode, and steady-state P_o, respectively. (*B*) Calcium dependence of the relative contribution of the three modes to channel activity expressed as probability of mode occurrence. ○, ⊕, ●, Values for modes I, L, and H, respectively, obtained by analysis of simulated data. Dotted, dashed, and full lines indicate the respective calcium dependencies calculated directly from rate constants.

Gating activity consisting of three modes (null-, low-, and high-open-probability modes I, L, and H, respectively) was apparent in the simulated records, as it was in the experiments. All three modes could be resolved at or above $[Ca^{2+}] = 0.5$ μM. For lower $[Ca^{2+}]$, it was not possible to discriminate between the high- and low-open-probability segments. Calcium dependencies of the mode properties were determined by single-channel analysis of simulated data using Eq. 3. Theoretical calcium dependencies were estimated from Eq. 2 using the rate constants from Table 1 and assuming that the H mode and the peak response arise from the fast subset of states (R, C1, O1) only, that the L-mode response arises from states C2 and O2, and that all states of the scheme participate in the steady-state open probability. The results from both approaches are given in Table 2 (see also *fitted curves* in Fig. 3). The open probability within the L mode was found to be independent of Ca^{2+}, whereas the open probability within the H mode increased with Ca^{2+}. The open probability during each of the active modes was much less variable than the overall open probability, as was the case with the experimental data (Zahradníková and Zahradník, 1995a).

The probability of occurrence of each mode was calcium dependent. Mode L and mode I were more prominent at high Ca^{2+}, whereas the probability of H-mode occurrence decreased with Ca^{2+}. There were significant variations between individual simulations regarding mode occurrence, which resulted mainly in variations of K_{Ca} for mode probabilities (Table 2), another feature of the model akin to experimental data.

Modal and burst analysis

To compare the model with experiments regarding the intramodal behavior, a set of 12 files, corresponding to the experimental set used by Zahradníková and Zahradník (1995a), was generated for 10 μM Ca^{2+} and analyzed using the same modal analysis technique. A comparison of the intramodal behavior as predicted by the model with the experimentally measured values is given in Fig. 4. In accordance with the experimental observations, two open times, three closed times, and two types of bursts could be detected in either open mode. Similarly, the values of lifetimes or number of openings per burst were not found to vary between mode types. The proportion of individual open and closed time components and the proportion of the two burst types was drastically different in mode L and mode H, as observed in experiments. It has to be noted that, in this model, the presence of two types of openings and two types of bursts in individual modes results from cross-contamination of the modes by short-lasting sojourns in the opposite active mode.

TABLE 2 Calcium dependence of open probabilities and probabilities of modes

		Probability		Calcium sensitivity, K_{Ca}	
		Simulated	Theoretical	Simulated	Theoretical
Steady-state P_o	$P_{o,steady}^{max}$	0.207 ± 0.006	0.214	1.11 ± 0.29	0.97
Within-mode P_o	$P_{o,L}$	0.028 ± 0.001	0.032	—	—
	$P_{o,H}^{max}$	0.597 ± 0.016	0.952	2.92 ± 0.25	4.76
Probability of mode occurrence	$P_{I,max}$	0.112 ± 0.06	0.194	0.99 ± 0.14	0.97
	P_L^{max}	0.570 ± 0.015	0.602	0.88 ± 0.12	0.97
	P_H^{max}	1.03 ± 0.13	1.0	1.40 ± 0.56	0.97
	P_H^{min}	0.31 ± 0.01	0.204		
Peak P_o	$P_{o,peak}^{max}$	0.914 ± 0.002	0.952	4.47 ± 0.06	4.76

$P_{o,L}$ is independent of Ca^{2+}; P_H is a decreasing hyperbolic function of Ca^{2+}. All other probabilities are increasing hyperbolic functions of Ca^{2+}.

The transitions between modes for the model were inspected using the nest-diagram technique (Zahradníková and Zahradník, 1995a) at several Ca^{2+} concentrations between 0.5 and 1000 μM (Fig. 5). In addition to documenting the Ca dependence of open probability in mode H, and its Ca independence in mode L, the nest diagrams illustrate the Ca dependence of the observable transition frequencies between modes. At low Ca^{2+}, transitions L ↔ H prevail, whereas transitions L ↔ I become more prominent at $[Ca^{2+}] > 5$ μM. Although the model states that no direct transitions between the H mode and I mode are possible, apparent H ↔ I transitions can be observed in the nest diagrams at Ca^{2+} concentrations above the steady-state K_{Ca}, albeit with a low probability, similar to what was observed experimentally (Zahradníková and Zahradník, 1995a). It is apparent that in the modeled case the presence of direct

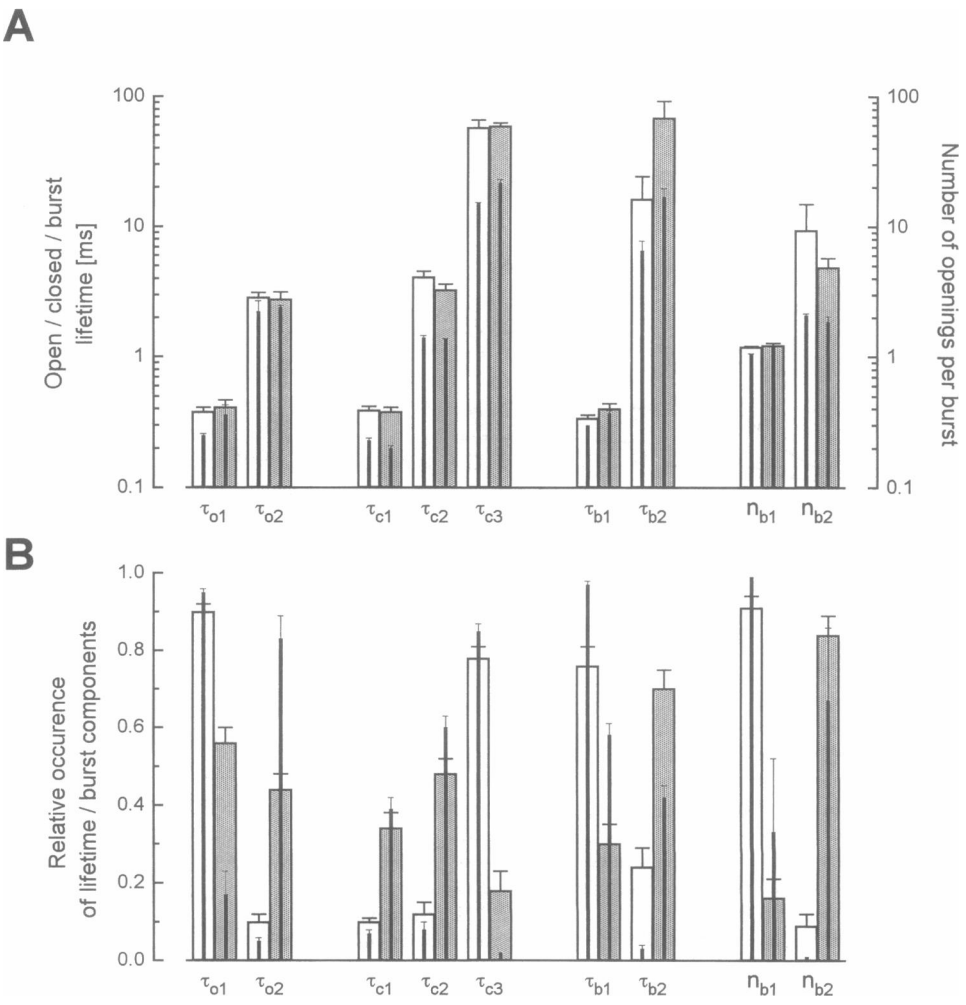

FIGURE 4 Open and closed times, and burst distributions in the two modes of activity. The lifetime parameters of channel kinetics in the two active modes (L mode, open bars; H mode, hatched bars) measured experimentally (Zahradníková and Zahradník, 1995a) are compared with the values obtained from simulated data analyzed in the same fashion (*rods*). (*A*) Values of open, closed, and burst lifetimes and numbers of openings per burst. (*B*) Relative areas of individual components of the distributions shown in *A*.

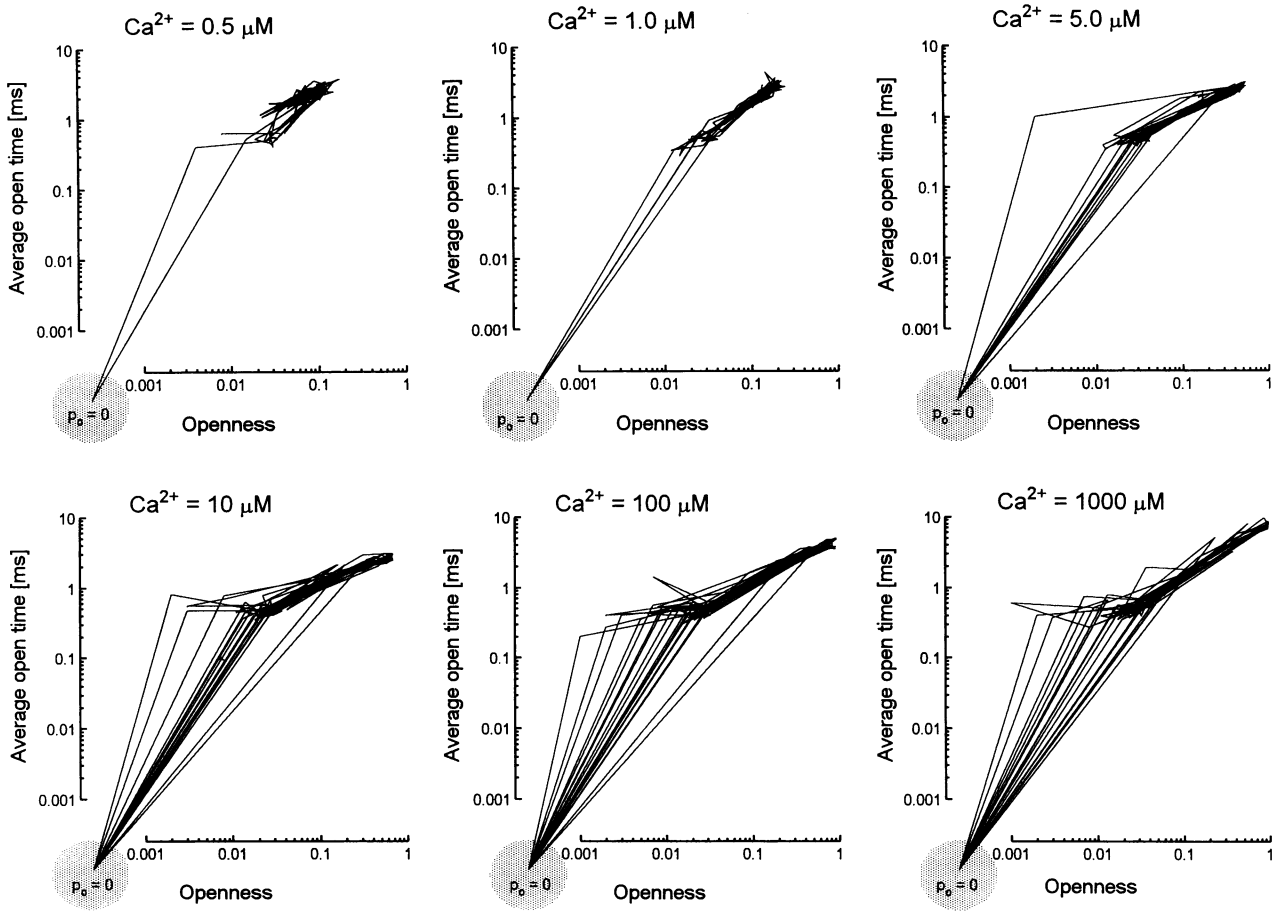

FIGURE 5 Calcium dependence of intermodal behavior in steady state. Nest diagrams of simulated channel activity (60 s each) at six selected Ca^{2+} concentrations, indicated above the diagrams. Nest diagrams are constructed by plotting the average open time within each segment against P_o of that segment and connecting the points from consecutive segments by lines.

H ↔ I transitions in the nest diagram was caused by cross-contamination of H and I modes by short-lasting sojourns in the low-probability mode L.

RESPONSES OF THE MODEL TO STEP CHANGES IN ACTIVATING Ca^{2+} CONCENTRATION

Simulations at the single-channel level

The model was based on data from single-channel responses in a narrow range of Ca^{2+} concentration steps (Györke and Fill, 1993). In this section we inspect the predictions of the model for the entire range of Ca steps, which are expected to occur during the E-C coupling process. Calcium steps from the resting level of 0.05 μM to concentrations of 0.5–1000 μM were used, as shown in Fig. 6 *A*. It is obvious that the channel behavior immediately after activation is markedly different from that in the steady state (cf. Fig. 2 *A*). The single-channel records exhibited bursts of closely spaced openings at the beginning of the step, whereas periods of lower activity and longer closures were observed at later times.

A set of 64 single-channel responses to a step change in calcium, such as that shown in Fig. 6 *A*, was simulated and then averaged. The ensemble open probabilities, obtained by dividing the average current by the single-channel amplitude (Fig. 6 *B*, *noisy traces*) showed transient activation consisting of a rapid rising phase followed by a slower decaying phase. Their time course was similar to the theoretical kinetics (Fig. 6 *B*, *full lines*), suggesting that the relatively high proportion of missed short openings did not significantly contribute to ensemble open probability. We analyzed the time course of distribution of modes in successive 409.6-ms segments after the calcium steps. At the beginning of the steps, the H mode was almost exclusively present, and its probability decayed with time in a calcium-dependent manner (Fig. 6 *B*, *circles*). On the contrary, occurrence of the L mode increased with time and saturated at values predicted by steady-state modal analysis, and the I mode, appearing with a delay, did not saturate within the time span of the records (data not shown). Properties of the modes (lifetime and burst parameters, within-mode open-probability) did not change with time after the Ca^{2+} step (not shown).

The overall kinetics of the transients was analyzed by fitting the time course of channel open probability, which

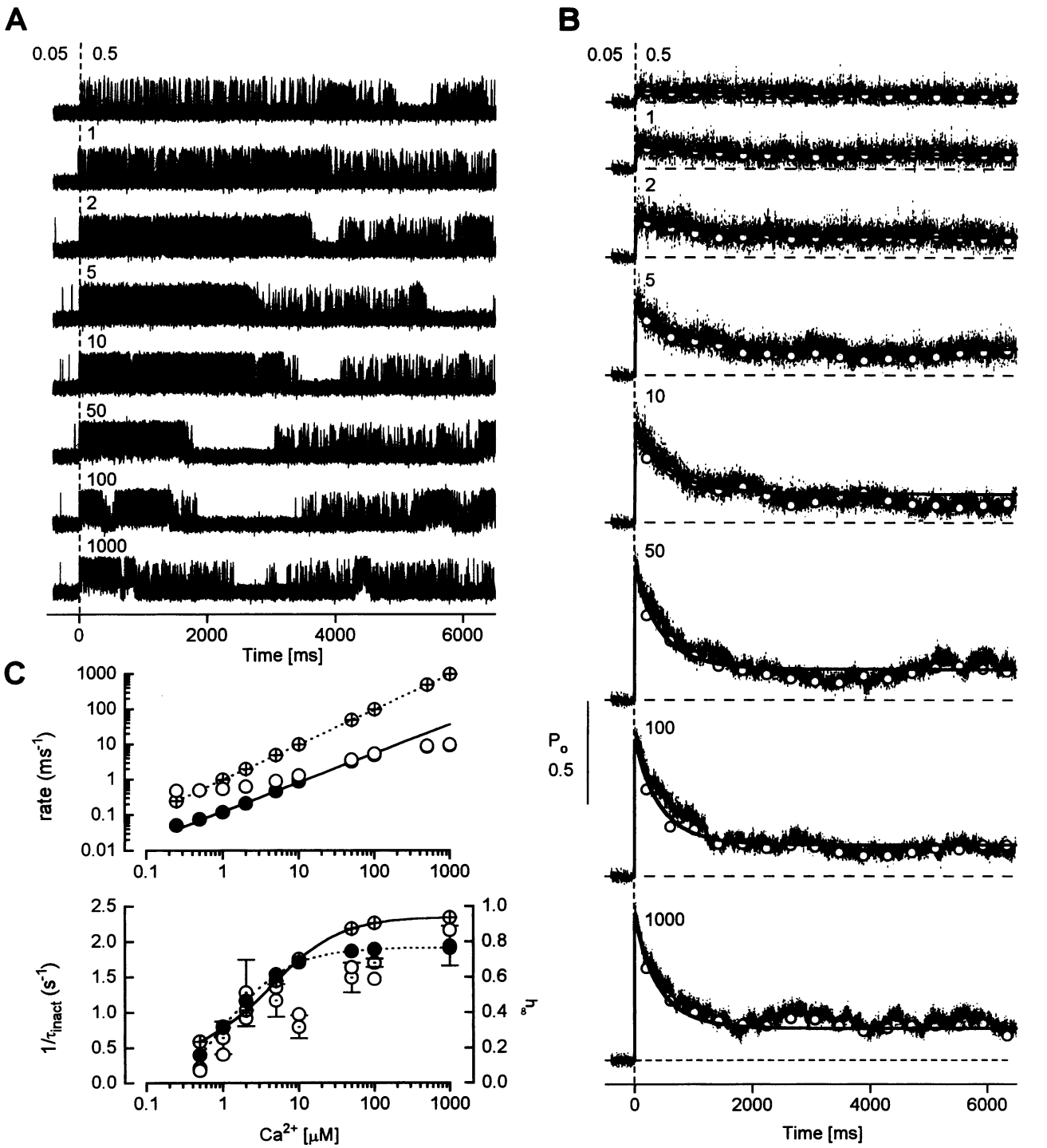

FIGURE 6 Transient responses of the model to step $[Ca^{2+}]$ changes. (*A*) Simulated single-channel traces after a step change from the resting 0.050 μM Ca^{2+} level to 0.5–1000 μM Ca^{2+} concentrations (indicated at the traces). (*B*) Ensemble open probability of simulated currents (*noisy traces*) under the same conditions as in *A*. Circles indicate the H-mode probabilities evaluated for consecutive 409.6-ms segments. The full lines represent the theoretical time course of the ensemble open probability. (*C*) Calcium dependence of the kinetic parameters. *Upper panel*: Dependence of the activation rate, $1/\tau_{act}$, before (○) and after (●) the correction for deactivation, $1/\tau_{act} - 1/\tau_{deact}$, shown together with the rate of Ca^{2+} binding to the channel ($k_{RC1} \times [Ca^{2+}]$; ⊕). The full and dotted fitted lines give a value of k_{on} for Ca^{2+} binding of 1.33×10^8 and 1.0×10^9 M^{-1} s^{-1}, respectively. *Lower panel*: Left axis, Calcium dependence of the inactivation rate, $1/\tau_{inact}$, obtained by fitting monoexponential functions to the theoretical responses (⊕), by fitting monoexponential functions to ensemble-averaged currents (○), and by fitting the decay of the H-mode probabilities (⊙). Right axis, Calcium dependence of the extent of inactivation (h_∞, ●). The full and dotted lines are spline functions connecting the crossed and full circles to enhance clarity.

was either calculated by numerical integration of the kinetic equations or obtained as the ensemble average of simulated records. In the range 0.5–1000 μM Ca^{2+}, both activation and inactivation time courses of theoretical/simulated channel activity could be fitted by monoexponential functions. The rate of activation increased more than 20 times from 455 s^{-1} at low to 11,000 s^{-1} at high Ca^{2+} (Fig. 6 *C*) and saturated as the C1 $\leftrightarrow$ O1 transition became rate-limiting instead of R $\leftrightarrow$ C1. This occurs in the same concentration range as Ca^{2+} activation of the channel in the H mode and its open probability at the peak of activity (Fig. 3 *A*, Table 2), confirming that the H mode as defined by analysis of steady-state records determines the activation of the channel.

Inactivation rate ($1/\tau_{inact}$) increased about 8 times from 0.26 s^{-1} at low to 2.23 s^{-1} at high Ca^{2+} (Fig. 6 *C*) and, interestingly, saturated at Ca^{2+} concentrations lower than the activation rate did. Saturation occurred when 1) the O1 $\leftrightarrow$ C2 transition became rate-limiting instead of C1 $\leftrightarrow$ O2, and 2) the maximum level of p_{O1} was reached, and therefore the concentration dependence of the inactivation rate (i.e., the Ca^{2+} range in which saturation occurred) was closer to that of steady-state P_o. As a result, the inactivation rates, when determined from the observable range of transient responses (which is for ideal records above 0.13 μM Ca^{2+}, and for sampled, noisy, and filtered records above 0.5 μM Ca^{2+}), will provide a maximally fourfold acceleration of inactivation. The extent of inactivation (h_∞) increased with Ca^{2+} from 0.16 at the Ca^{2+} step of 0.5 μM up to its maximum value of 0.77 at 50 μM and larger Ca^{2+} steps, with a concentration dependence very close to one of $1/\tau_{inact}$ (Fig. 6 *C*).

Responses of the model to repeated stimuli

An important aspect of the cardiac calcium release channel gating observed experimentally (Györke and Fill, 1993) is the ability to activate repeatedly in response to cumulative stimuli, termed adaptation. First we have evaluated the theoretical time course of open probabilities for Ca^{2+} prepulses of variable duration and height, followed by test pulses to 0.5, 1, 2, and 5 μM Ca^{2+}, the concentration range used by Györke and Fill (1993). Activation and inactivation rates during the test pulse were not affected by the prepulse amplitude or duration (not shown) and were identical to rates of controls (Fig. 6 *B*), as can be expected from the monoexponential time course of inactivation. Peak open probability during the test pulse was partially inactivated by a Ca^{2+} prepulse. $P_{o,peak}$ decreased with increasing prepulse duration and with increasing prepulse Ca^{2+} concentration (Fig. 7 *B*). Prepulses to the same absolute Ca^{2+} level decreased $P_{o,peak}$ in test pulses to different Ca^{2+} levels to approximately the same extent, and responses to higher test pulses were slightly more sensitive to inactivation by a prepulse. Suppression of $P_{o,peak}$ developed with an approximately monoexponential time course, with time constants decreasing with increasing [Ca^{2+}] of the prepulse, providing a K_{Ca} for peak suppression of 0.99 μM. When the Ca^{2+} prepulse amplitude was kept constant, the rate of $P_{o,peak}$ suppression slightly increased with the test pulse Ca^{2+} concentration.

The model provides transient responses to a series of Ca^{2+} increments over a wide range of Ca^{2+} concentrations (Fig. 7 *C*, *solid line*). The pattern of the response resembles the "increment detection behavior" (Meyer and Stryer, 1990). As can be seen from the figure, transient responses can be induced only at Ca^{2+} higher than 0.13 μM (in accord with the value specified in the section "Construction of the model") throughout the Ca^{2+} range, as long as the pool of state R is not exhausted (*dotted line*). The increase in open probability is proportional to the decrease in state R probability at a given step (Fig. 7 *D*, *squares*). According to this model the "increment detection behavior" results from inactivation of a subset of channels recruited by Ca^{2+} from the available pool of resting channels. At the level of a single channel the increment detection can be observed while the channel resides within H-mode states (R, C1, O1) at the instant of Ca^{2+} concentration change, and is manifested as the increase in $P_{o,H}$ after the step, followed by redistribution of probabilities of modes into a new steady state. Therefore the increase in the ensemble-averaged P_o is proportional to the product of probability of H mode (P_H) before the step and open probability within H mode ($P_{o,H}$) after the step (Fig. 7 *D*, *circles*; calculated using the values from Table 2).

Response of the model to a step decrease in Ca^{2+}

Describing the inactivation mechanism of the model brings about the logical question, what will be the prediction of the present model for the recovery from inactivation, which is expected to happen on resuming the resting level of free Ca^{2+} in the junctional space? The kinetics of channel deactivation from the steady-state activity after a step decrease in Ca^{2+} was analyzed for backward steps to the 0.05 μM Ca^{2+} level from a range of initial activating concentrations (1 to 1000 μM). The decrease in channel activity was found to be biexponential, independently of the preactivating Ca^{2+} level. First 95% of the open probability decayed with a time constant of 2.35 $\pm$ 0.29 ms (the theoretical value being 2.18 ms), suggesting that the fast phase of deactivation corresponds to channel closure within H mode, and the remaining 5% decayed with a time constant of 2.7 $\pm$ 1.5 s (the theoretical value was 1.72 s). The single-channel activity during the decay phase is illustrated in Fig. 8 for a step from 1000 to 0.05 μM Ca^{2+}. The fast decay phase consisted on average of at most one opening from the longer open time distribution. The slow phase of channel deactivation was characterized by L-mode-type activity, i.e., short openings separated by longer closures (Fig. 8 *A*, *left panel*), which strongly differs from the steady-state activity at 0.05

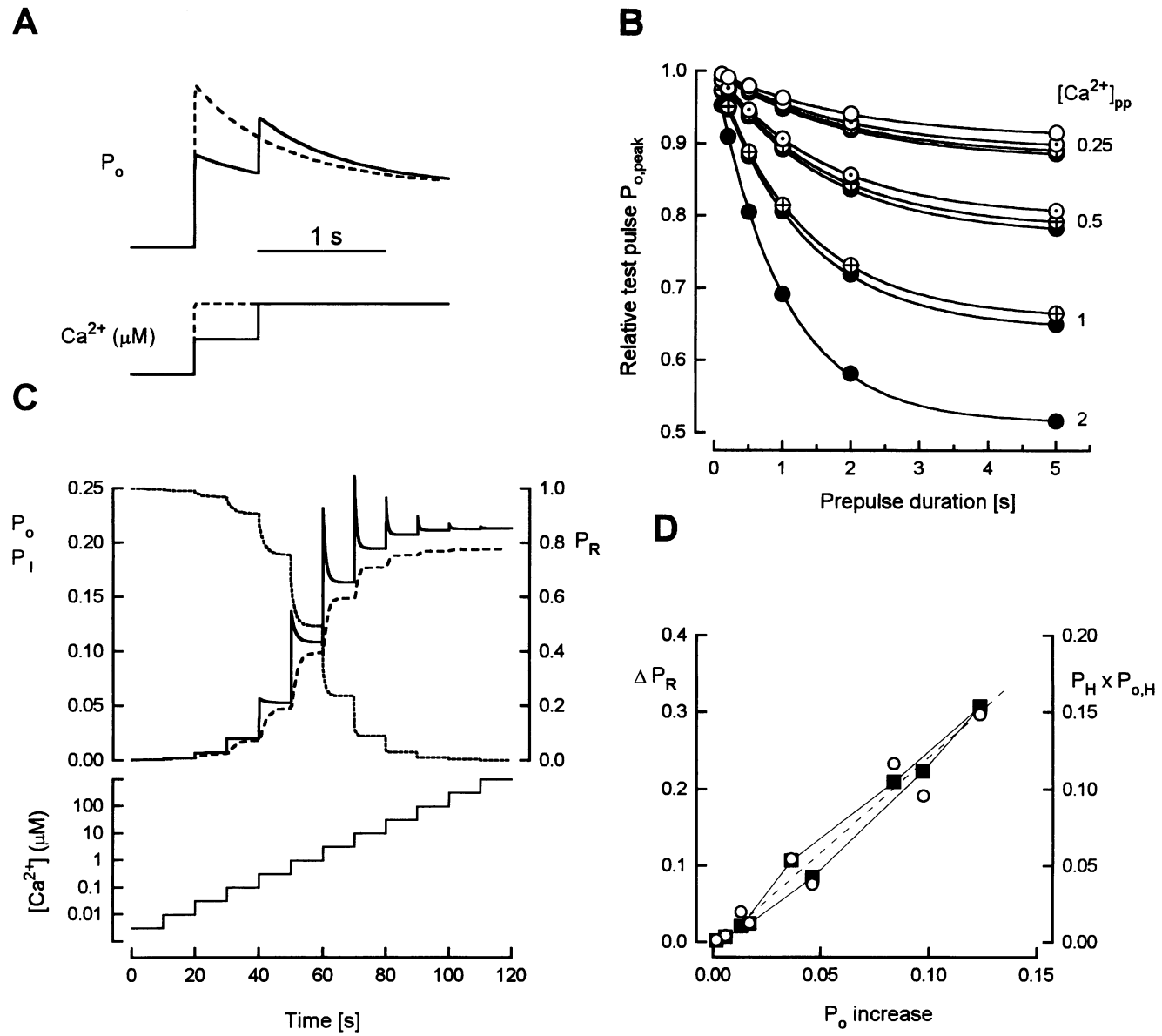

FIGURE 7 Incremental activation of the Ca release channel. (*A*) Example of the modeling experiment evaluated in *B*. *Top*: Superposition of the ensemble open probability time courses in response to the step changes of activating Ca concentration in single Ca^{2+} pulse (control, – – –) and in the two-step Ca^{2+} increments (——). *Bottom*: Activation protocols: single Ca^{2+} concentration pulse (– – –) of the control experiment, and prepulse and test pulse (——) in the two-step Ca^{2+} increments. (*B*) Evaluation of experiments outlined in *A*. Dependence of the test pulse $P_{o,peak}$ on duration (*abscissa*) and Ca^{2+} level of the prepulse ($[Ca^{2+}]_{pp}$, indicated at the right side in μM) relative to the control single pulse experiment. ○, ⊙, ⊕, ●, Test pulse Ca^{2+} concentrations of 0.5, 1, 2, and 5 μM, respectively. (*C*) Response of the model channel to sequential steps of Ca^{2+} concentrations spanning the whole range from 10^{-9} to 10^{-3} M. *Top*: Ensemble open probability (*full line, left axis*), probability of the resting state (*dotted line, right axis*), and probability of mode I (*dashed line, left axis*). *Bottom*: Ca^{2+} concentration profile. (*D*) The relationship between the P_o increase (*abscissa*) and either the decrease in probability of the resting state ΔP_R (■, *left axis*), or the product of pre-step P_H and post-step $P_{o,H}$ probabilities (○, *right axis*), with linear regression shown as dotted line, $R = 0.993$.

μM Ca^{2+}, in which isolated long openings dominate (*right panel*). Although in the steady state at 0.05 μM Ca^{2+} the L and H modes cannot be distinguished from each other (see "Ca^{2+} dependence of P_o and modes"), L-mode-type activity can be disclosed to underlie the slow phase of deactivation. The average open time was 0.75 ± 0.06 ms in segments starting at 10 ms after the Ca^{2+} decrease (i.e., after the fast phase of deactivation was well over) and lasting 400 ms, whereas the steady-state average open time was 2.19 ± 0.13 ms. The average open probability during the slow phase of decay was at the same time 0.026 ± 0.001 in segments containing openings (cf. the calcium-independent value of 0.028 ± 0.001 for L mode in Table 2), whereas the steady-state open probability for the opening-containing segments was 0.012 ± 0.001 (cf. the theoretical $P_{o,L} + P_{o,H} = 0.015$ for Ca^{2+} = 0.05 μM calculated from Table 2 data). The

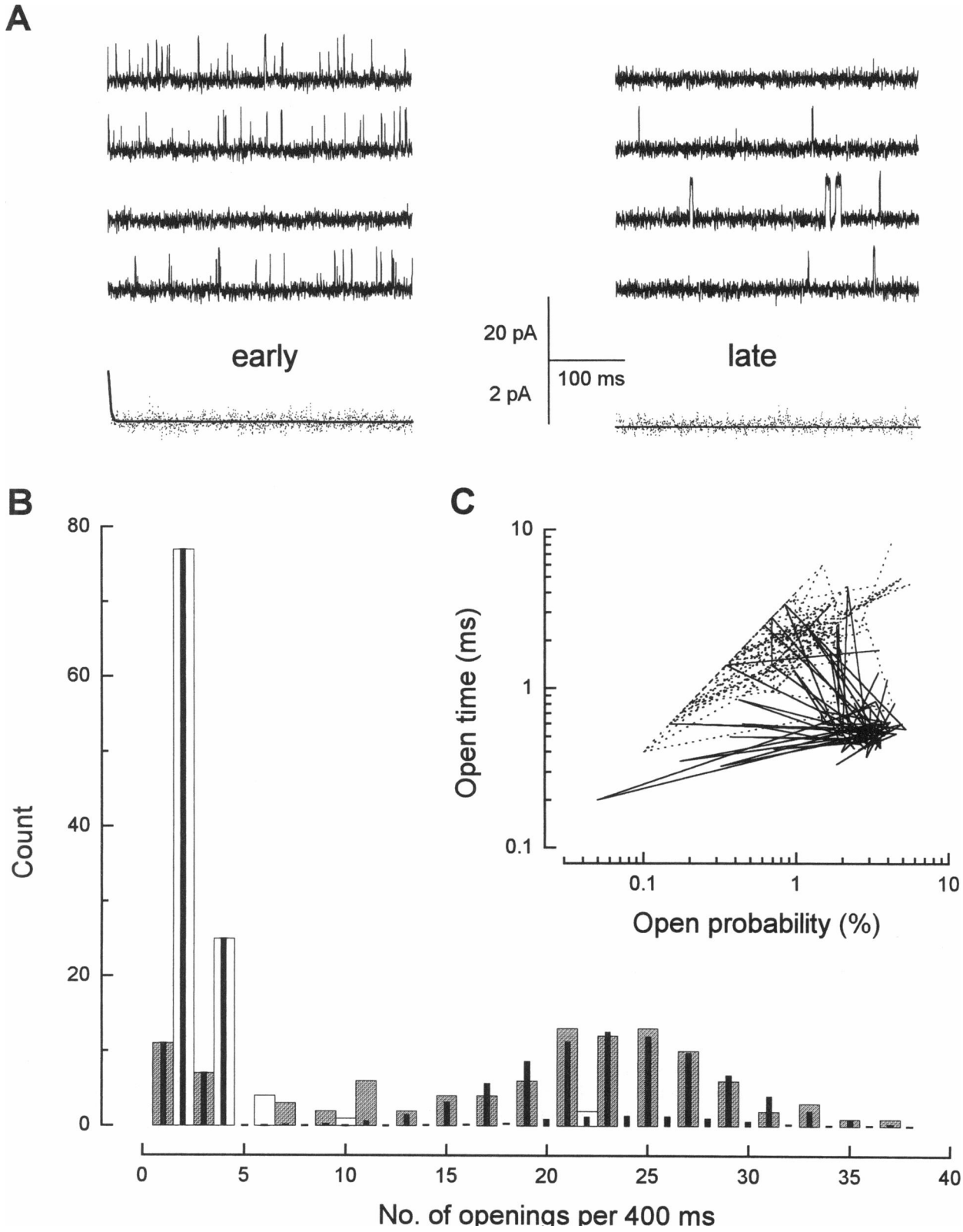

FIGURE 8 Single-channel activity after a step decrease in Ca^{2+}. (*A*) Segments (400 ms) of activity immediately after (*left*) and 3 s after (*right*) a step decrease in Ca^{2+} from 1000 to 0.05 μM. The bottom trace is an average of 128 simulated single-channel records (note the difference in scale). (*B*) The distribution of the opening frequencies for the simulation shown in *A*. To avoid superposition of the columns, the column width was reduced to one-half of the bin with, and the slow phase of deactivation is shown at right (*gray bars*), and the steady state is shown at left (*hollow bars*). The respective theoretical distributions are superimposed (*thick lines*). (*C*) Nest diagram of the early (*full line*) and late (*dotted line*) phase. The values obtained in consecutive repeated simulations are shown as a line plot to enhance clarity .

differences in population of L mode between the late phase of deactivation and the steady state are also apparent from their respective opening frequencies (Fig. 8 *B*), which are bimodal and differ in the proportions of the two Gaussian components corresponding to the two active modes. The nest diagram (Fig. 8 *C*) illustrates these different patterns of activity, visualizes the properties of both active modes, and shows that the inability to discern between H mode and L mode in the steady state is caused by the very low probability of L mode at low Ca^{2+} concentration. The pattern of the decay phase activity is similar in the whole range of preactivating Ca^{2+}, but the differences between the slow phase of deactivation and the steady state become less prominent at lower values of preactivating Ca^{2+}, which is consistent with the lower probability of L-mode occurrence under these conditions.

DISCUSSION

The presented analysis of the Ca release channel gating model has shown that the model meets the criteria used for its construction and successfully simulates many features of the real experiments. Therefore, it represents a useful tool for testing hypotheses and designing experiments.

The basic assumptions of this model were that among the three modes of activity (Zahradníková and Zahradník, 1995a), only the H mode is directly accessible from the resting state, and, because of the rapidity and high proportion of R $\leftrightarrow$ C1 transitions at Ca^{2+} levels above the binding constant, the resting state can be regarded as a part of the H-mode states. These assumptions result in the predicted Ca^{2+} dependencies of the steady-state properties of the modes, namely: 1) Open probability within the H mode increases with Ca^{2+}, whereas P_o within the L mode is Ca^{2+}-independent. 2) The probability of the H-mode occurrence decreases, whereas probabilities of the L mode and I mode increase with Ca^{2+}. 3) The Ca^{2+} sensitivity of mode probability, equal for all three modes, coincides with the Ca^{2+} dependence of the steady-state open probability. Experimental verification of these predictions, which hold generally for all analogous models, could provide a stringent answer regarding the validity of this class of models for CRC gating.

Another direct consequence of our basic assumptions is the exact correspondence between channel activity early after activation (at the peak of open probability) and its activity within H-mode sojourn in the steady state. This prediction can be experimentally tested as well, and the approach of modal analysis (Zahradníková and Zahradník, 1995a) used together with the techniques we introduced here could be effectively used for the purpose.

Modeling of steady-state activity

As can be expected from the gating scheme, the model generates two open times of invariable relative contribution to the open probability over the whole Ca^{2+} range (<1000 μM) inspected, in accordance with most published experimental data (Ashley and Williams, 1990; Chu et al., 1993; Sitsapesan and Williams, 1994; Zahradníková and Zahradník, 1995a). At high calcium, the increasing number of missed very short closures begins to influence both the measurement of open times (artificial prolongation of the longer open time component up to appearance of a false third open time component) and the estimation of their relative contribution (deviation from the theoretical prediction becomes significant). This observation of the simulated data warns of premature conclusions on the number of open or closed times estimated by fitting routines more "powerful" than the data.

The model predicts four closed time constants, of which only that corresponding to the state R (τ_{c4}) is Ca-dependent and changes over four orders of magnitude. We managed to resolve all closed time components only at several of the investigated Ca^{2+} concentrations. The collection of huge numbers of events, a procedure that cannot be easily achieved in real experiments, was necessary. These modeling results explain differences among several laboratories in describing changes of closed and open times with Ca^{2+}, and in attribution of the channel open probability changes with increasing Ca^{2+} to changes in the proportion of the individual time components (Chu et al., 1993; Zahradníková and Palade, 1993; Zahradníková and Zahradník, 1995a). As a result of the fast binding of calcium to the channel, and the channel sensitivity to Ca^{2+} in the micromolar range, the closed time component corresponding to the state R is dominant and consequently overshadows components with similar time constants. Resolving these components at low Ca^{2+} is further impeded by infrequent openings of the channel. Calcium-dependent coincidence of the variable component τ_{c4} with either the slow, the medium, or the fast components gives rise to apparent Ca^{2+} dependence of the measured relative areas W_i of these three Ca-independent time constants. Previously we argued (Zahradníková and Zahradník, 1995a) that the lack of the obvious Ca dependence of the experimentally observed closed time constants results from the limited time resolution of the measurements, as the rapid Ca^{2+}-dependent transitions may be filtered out. This holds for the presented model at $Ca^{2+} >$ 10 μM. Finally, the finding that a substantial proportion of the longest closed time component is still present at high calcium concentration, which is essential for our model and provides the rationale for existence of the inactivated state, is also in agreement with the published reports.

Still, even in this simple model and under conditions favorable over the experiments (fair signal-to-noise ratio, long simulations), the errors in the estimated values of τ_i and W_i due to missing of both brief openings and closures, were significant, despite the very thorough analysis (cf. Fig. 2 *B*). Accordingly, we are skeptical that without a significant improvement in the time resolution of experiments it will be possible to gain a deeper insight into the fast RyR channel gating, especially its Ca^{2+} ion-binding steps. On

the other hand, far fewer data were necessary for modal analyses than for analysis of fast channel gating to obtain statistically reliable results. Modal analyses performed on steady-state experimental data, even with the recent methodological state-of-the-art technique, therefore could still add to our understanding of CRC gating.

Analysis of the simulated data has confirmed that noise and filtering, as well as the finite length of the segment, introduce errors into modal analysis (Zahradníková and Zahradník, 1995a) that are similar to errors introduced in event analysis (Wilson and Brown, 1985). In this respect a segment is analogous to a sample point and individual modes are analogous to individual channel states. This type of error was manifested as the presence of short openings within the H mode (Fig. 4) and the presence of the false direct H ↔ I transitions (Fig. 5).

Dynamic behavior of the model

The dynamic aspects of channel gating, the so-called adaptive behavior observed by Györke and Fill (1993), are very well reproduced by the model at Ca^{2+} concentrations higher than 1 μM. At lower Ca^{2+} the responses of the channel did not show a prominent inactivation phase and were more similar to the recent findings of Schiefer et al. (1995) obtained by the liquid filament technique of changing Ca^{2+} concentration. Both the rapid activation and a much slower inactivation are monoexponential processes with time constants decreasing with increasing Ca^{2+} concentration in a saturable manner. The Ca^{2+} dependence of the rates of activation and inactivation, as well as that of the extent of inactivation, is in very good agreement with the values experimentally determined by Schiefer et al. (1995). Interestingly, the apparent calcium sensitivity of the activation rate is less than that of inactivation rate. According to our model, however, this does not result from different Ca^{2+} binding sites responsible for activation and inactivation, but it is rather a consequence of the different rate-limiting transitions between sets of states, or in other words, different absorbing states (O1 for activation, O2 and I for inactivation; Colquhoun and Hawkes, 1982).

The rate of deactivation predicted upon Ca withdrawal was found to be independent of the Ca^{2+} level, as can be expected. Less expected was the observation that 95% of deactivation proceeds with a time constant of 2 ms, a value very close to the value of ~5 ms reported by Schiefer et al. (1995). During deactivation from high Ca^{2+} concentrations Schiefer et al. (1995) also observed a slow phase of current decline with a time constant of 842 ms, a value not far from the prediction of our model, which was not detectable at lower Ca^{2+} values, again in accordance with our model.

Modal analysis revealed that clusters of the H-mode activity appear at the onset of the [Ca^{2+}] pulses, whereas the L and I modes dominate the ends of records, thus endorsing our previous hypothesis (Zahradníková and Zahradník, 1995a). This hypothesis was experimentally confirmed recently by resolving the transitions between modes of channel activity during adaptation, by the prevalence of the H mode at the peak of open probability (Zahradníková et al., 1996), and by the finding of Schiefer et al. (1995) that the average open time within the first 200 ms after activation is on the order of 2 ms and more, as is the value typical for the H mode. The high probability of the I mode at high Ca^{2+} concentrations might also explain the refractoriness of the channel observed by Schiefer et al. (1995) during fast switching between pCa > 8 and pCa = 3.

The model has the potential to explain observations in the release experiments with SR vesicles. For cumulative [Ca^{2+}] stimuli, the model simulates the "increment detection" (Meyer and Stryer, 1990) response. According to our model, the mechanism of increment detection can be conceived simply as a gradual recruitment of channels by an agonist from the instant pool of agonist-free (resting state) channels, always passing through the H mode before reaching the steady-state inactivation (which may vary among channels or agonists according to the respective equilibrium constants).

Other predictions of the model

The model predicts several other characteristics of the transient behavior of the channel during responses to rapid changes of the activating Ca^{2+} concentration, which could be experimentally tested.

–A surge in Ca^{2+} from the adjoining L-type Ca channel, which was estimated by Rose et al. (1992) to produce an increase in Ca^{2+} to > 10 μM lasting for ~0.6 ms, should produce on average at most one opening of the CRC lasting ~2.5 ms (the average open time within the H mode). Whether this prediction is true can be tested with the help of the high-affinity caged Ca^{2+} compounds (DM-nitrophen or NP-EGTA) to produce Ca^{2+} spikes (Escobar et al., 1995; Ellis-Davies et al., 1996) of amplitude and duration comparable to injection via the L-type Ca channel.

–In two-pulse experiments the level and duration of the [Ca^{2+}] prepulse modulates only the amplitude of the P_o transient during the test pulse, without affecting its activation and inactivation rates.

–The intramodal characteristics of the L mode do not change with either time after the Ca^{2+} step or the level of Ca^{2+} attained. On the other hand, the within-mode open probability and intramodal closed times of the H mode do change with Ca^{2+}, but they are predicted to be invariant in time after a step Ca^{2+} change.

Comparison with other models of calcium release channel gating

Other recently published models, designed specifically to reproduce different aspects of the adaptation phenomena, predict single-channel behavior different from the experimental observations. The model of Tang and Othmer (1994)

incorporates a calcium-dependent inactivation step, and therefore it incorrectly predicts a decrease in single-channel activity in the steady state to zero at $[Ca^{2+}] \geq 10\ \mu M$. In the models of Cheng et al. (1995) and Sachs et al. (1995), individual open states differ in the number of bound Ca^{2+} ions, and therefore their proportions are strongly dependent on Ca^{2+} concentration. The model of Sachs et al. (1995) predicts significant activation of the channel in the absence of an activator, and prolongation of one of the open times with increasing Ca^{2+}. The model of Cheng et al. (1995) incorporates a large number of open states, comparable to the number of closed states, with lifetimes that are Ca^{2+} dependent. Neither of those predictions has real support in experimentally observed single-channel activity.

Schiefer et al. (1995) suggest three Ca^{2+}-binding sites to interpret the time and calcium dependence of CRC open probability, based on the calcium dependence of inactivation rate and the occurrence of slow reopenings and the slow deactivation phase. However, their data, specifically the increase in the inactivation rate and in its extent with increasing Ca^{2+}, the existence of the slow phase of deactivation during which reopenings of an "inactivated" channel occur, and rates of activation and deactivation, can all be simulated very reliably with our one Ca binding site model (see the section "Dynamic behavior of the model," and Figs. 6 and 8). It should be noted that the results of Schiefer et al. (1995) were not available to us at the time of the model construction. It should also be noted that the wide separation in the rate of the fast and the slow processes does not necessarily ensure that a simplified analysis, as used by Schiefer et al. (1995), will produce correct results. For instance, analysis of our model by the method of Schiefer et al. (1995) yields a value of $1.33 \times 10^8\ M^{-1}\ s^{-1}$ for k_{on}, whereas the correct value is almost 10 times larger (see Fig. 8 and Table 1). One would obtain a still higher difference between the calculated and the correct values of k_{off} ($1/\tau_d = 457\ s^{-1}$, whereas $k_{C1R} = 1.0 \times 10^5\ s^{-1}$, respectively; see Table 1). Because in the presented model binding of a single Ca^{2+} ion produces results compatible with the experimental observations, i.e., it shows different calcium sensitivities of peak and steady-state open probability and different apparent calcium sensitivities of activation and inactivation rate, these differences cannot be used as a sound evidence for the presence of different Ca^{2+}-binding sites. Instead, we suggest that these differences arise simply from the involvement of different sets of the channel's states in the respective responses, not necessarily differing in the number of bound Ca^{2+} ions.

Peak versus steady-state calcium sensitivity of the open probability

The apparent K_{Ca} estimated from the peak and from the steady-state P_o were found (Györke and Fill, 1993) to be significantly different, i.e., the peak response was about 5 times more sensitive to Ca^{2+} than the steady-state response, when measured by the caged Ca^{2+} technique. Our model, although reproducing other experimental aspects very well, predicts the opposite shift, i.e., that the apparent K_{Ca} of peak P_o is about a factor of 4 higher than the apparent K_{Ca} of steady-state P_o. This results in another difference between our model and the observations—whereas in our model the difference between the peak and the steady-state open probability becomes most prominent at steps to high Ca^{2+}, it was observed by Györke and Fill (1993) to be most prominent at low Ca^{2+} steps. In this respect it should be noted that when the fast perfusion technique is used to change the Ca^{2+} concentration, neither inactivation at low Ca^{2+} nor a shift in K_{Ca} has been demonstrated (Schiefer et al., 1995), and in some studies, inactivation has not been detected at all (Sitsapesan et al., 1995). On the other hand, prominent calcium release adaptation has been observed at low agonist concentrations in experiments utilizing sarcoplasmic reticulum vesicles (Dettbarn et al., 1994; Mészáros et al., 1996) or even in living cells (Yasui et al., 1994; Györke and Györke, 1996).

There are still three points to be discussed regarding the discrepancy between the results of caged-Ca^{2+} experiments and our model. First, the changes in calcium concentration in the experiments of Györke and Fill (1993) could have been calcium spikes rather than steps, as argued by Lamb et al. (1994) and Lamb and Stephenson (1995). Our analysis of the problem (data not shown) indicates that calcium spikes of the size and shape suggested by Lamb and co-workers would shift the K_{Ca} for $P_{o,peak}$ of our model to or even below the experimentally observed values. However, the model then shows a very fast activation even at the lowest calcium steps, in contradiction to the observation (Györke and Fill, 1994; Györke et al., 1994). Lack of adaptation observed in analogous experiments with purified CRC by Vélez et al. (1995), and the rapid deactivation of the channel observed when Ca^{2+} was rapidly decreased by photolysis of the caged calcium buffer diazo-3 (Vélez et al., 1996), also make this explanation unlikely. In addition, recent measurement of the time course of calcium spikes, utilizing the fast Ca^{2+} indicator calcium orange (Escobar et al., 1995; Ellis-Davies et al., 1996), suggest that the spikes are much too fast to account for the observed phenomenon. Second, the channel activity might be additionally regulated by external calcium-binding molecules, or by external molecules stabilizing slow-access states of the channel (memory molecules). A model of this kind has been proposed to explain the increment detection behavior of the IP_3 receptor (Swillens, 1992). Possible regulation of this type is supported by the report of Vélez et al. (1995), who found that purified ryanodine receptors do not exhibit the decaying phase of activity after a step increase in Ca^{2+} concentration. Third, our model may be oversimplified and the observed shift in K_{Ca} of the peak open probability with respect to steady-state P_o might be a genuine property of the CRC. It has been shown that models with multiple binding sites might simulate this shift (Cheng et al., 1995), although they do not reproduce the observed return of open probability to resting levels at

the lowest Ca^{2+} steps (Györke and Fill, 1993). It has been demonstrated that a very large number of Ca^{2+}-binding sites is necessary to describe this phenomenon in terms of a thermodynamically reversible channel model (Stern, 1996).

More complex models may in a certain range of activating calcium concentrations provide both the modal behavior of the channel and the shift in calcium sensitivity observed during adaptation, e.g., a modification of the model of Cheng et al. (1995), where occupation of the activation and adaptation sites by calcium would be regarded not as transitions between open and closed states but as transitions between modes. Furthermore, extensions of our model, e.g., in which interaction of the channel with the regulatory molecule would change the proportions of the three channel modes at equilibrium, could possibly explain all of the mentioned findings. Models of this type are intriguing candidates, given the tetrameric nature of the ryanodine receptor and its numerous regulatory mechanisms. However, any refinement of the models desperately needs better experimental data.

The authors wish to express their thanks to S. Györke, L. G. Mészáros, E. Ríos, and I. Stavrovský for stimulating discussions and for valuable suggestions about theoretical aspects of this work, and to G. Droogmans for comments on the manuscript.

The research of AZ was supported in part by an International Research Scholar's award from the Howard Hughes Medical Institute, and that of IZ by grant VEGA 1203.

REFERENCES

Ashley, R. H., and A. J. Williams. 1990. Divalent cation activation and inhibition of single calcium release channels from sheep cardiac sarcoplasmic reticulum. *J. Gen. Physiol.* 95:981–1005.

Cannell, M. B., H. Cheng, and W. J. Lederer. 1994. Spatial non-uniformities in $[Ca^{2+}]$ during excitation-contraction coupling in cardiac myocytes. *Biophys. J.* 67:1942–1956.

Cannell, M. B., H. Cheng, and W. J. Lederer. 1995. The control of calcium release in heart muscle. *Science.* 268:1045–1049.

Cheng, H., M. Fill, H. Valdivia, and W. J. Lederer. 1995. Models of Ca^{2+} release channel adaptation. *Science.* 267:2009–2010.

Chu, A., M. Fill, E. Stefani, and M. L. Entmann. 1993. Cytoplasmic Ca^{2+} does not inhibit the cardiac muscle sarcoplasmic reticulum ryanodine receptor Ca^{2+} channel, although Ca^{2+}-induced Ca^{2+} inactivation of Ca^{2+} release is observed in native vesicles. *J. Membr. Biol.* 135:49–59.

Colquhoun, D., and A. G. Hawkes. 1982. On the stochastic properties of bursts of single ion channel openings and of clusters of bursts. *Philos. Trans. R. Soc. Lond. Biol.* 300:1–59.

Colquhoun, D., and A. G. Hawkes. 1983. The principles of the stochastic interpretation of ion channel mechanisms. *In* Single Channel Recording. B. Sakmann and E. Neher, editors. Plenum Press, New York. 135–175.

Coronado, R., J. Morrissette, M. Sukhareva, and D. M. Vaughan. 1994. Structure and function of ryanodine receptors. *Am. J. Physiol.* 266: C1485–C1504.

Dettbarn, C., S. Györke, and P. Palade. 1994. Many agonists induce "quantal" Ca^{2+} release or adaptive behavior in muscle ryanodine receptors. *Mol. Pharmacol.* 46:502–507.

Eberhard, M., and P. Erne. 1989. Kinetics of calcium binding to fluo-3 determined by stopped-flow fluorescence. *Biochem. Biophys. Res. Commun.* 163:309–314.

Ellis-Davies, G. C. R., J. H. Kaplan, and R. J. Barsotti. 1996. Laser photolysis of caged calcium: rates of calcium release by nitrophenyl-EGTA and DM-nitrophen. *Biophys. J.* 70:1006–1016.

Escobar, A. L., F. Cifuentes, and J. L. Vergara. 1995. Detection of Ca^{2+} transients elicited by flash photolysis of DM-nitrophen with a fast calcium indicator. *FEBS Lett.* 364:335–338.

Escobar, A. L., J. R. Monck, J. M. Fernandez, and J. L. Vergara. 1994. Localization of the site of Ca^{2+} release at the level of a single sarcomere in skeletal muscle fibres. *Nature.* 367:739–741.

Fabiato, A. 1985. Time and calcium dependence of activation and inactivation of calcium-induced calcium release of calcium from the sarcoplasmic reticulum of a skinned canine cardiac Purkinje cell. *J. Gen. Physiol.* 85:247–289.

Györke, I., and S. Györke. 1996. Adaptive control of intracellular Ca^{2+} release in C2C12 mouse myotubes. *Pflügers Arch.* 431:838–843.

Györke, S., and M. Fill. 1993. Ryanodine receptor adaptation: control mechanism of Ca^{2+}-induced Ca^{2+} release in heart. *Science.* 260: 807–809.

Györke, S., and M. Fill. 1994. Ca^{2+}-induced Ca^{2+} release in response to flash photolysis. *Response Sci.* 263:987.

Györke, S., P. Vélez, B. Suárez-Isla, and M. Fill. 1994. Activation of single cardiac and skeletal ryanodine receptor channels by flash photolysis of caged Ca^{2+}. *Biophys. J.* 66:1879–1886.

Klein, M. G., H. Cheng, L. F. Santana, Y.-H. Jiang, W. J. Lederer, and M. F. Schneider. 1996. Two mechanisms of quantized calcium release in skeletal muscle. *Nature.* 379:455–458.

Lamb, G. D., M. W. Fryer, and D. G. Stephenson. 1994. Ca^{2+}-induced Ca^{2+} release in response to flash photolysis. *Science.* 263:986–987.

Lamb, G. D., and D. G. Stephenson. 1995. Activation of ryanodine receptors by flash photolysis of caged Ca^{2+}. *Biophys. J.* 68:946–948.

López-López, J. R., P. S. Shacklock, C. W. Balke, and W. G. Wier. 1995. Local calcium transients triggered by single L-type calcium channel currents in cardiac cells. *Science.* 268:1042–1045.

Mészáros, L. G., A. Zahradníková, and I. Minarovič. 1996. The mechanism of quantal calcium release from intracellular calcium stores and release channel adaptation. *Biophys. J.* 70:A146.

Meyer, T., and L. Stryer. 1990. Transient calcium release induced by successive increments of inositol 1,4,5-trisphosphate. *Proc. Natl. Acad. Sci. USA.* 87:3841–3845.

Rios, E., and G. Brum. 1987. Involvement of dihydropyridine receptors in excitation-contraction coupling in skeletal muscle. *Nature.* 325: 717–720.

Rose, W. C., C. W. Balke, W. G. Wier, and E. Marban. 1992. Macroscopic and unitary properties of physiological ion flux through L-type Ca^{2+} channels in guinea-pig heart cells. *J. Physiol. (Lond.).* 456:267–284.

Sachs, F., F. Qin, and P. Palade. 1995. Models of Ca^{2+} release channel adaptation. *Science.* 267:2010–2011.

Schiefer, A., G. Meissner, and G. Isenberg. 1995. Ca^{2+} activation and Ca^{2+} inactivation of canine reconstituted cardiac sarcoplasmic reticulum Ca^{2+}-release channels. *J. Physiol. (Lond.).* 489:337–348.

Shacklock, P. S., W. G. Wier, and C. W. Balke. 1995. Local Ca^{2+} transients (Ca^{2+} sparks) originate at transverse tubules in rat heart cells. *J. Physiol. (Lond.).* 487:601–608.

Sitsapesan, R., and A. J. Williams. 1994. Gating of the native and purified cardiac SR Ca^{2+}-release channel with monovalent cations as permeant species. *Biophys. J.* 67:1484–1494.

Sitsapesan, R., R. A. P. Montgomery, and A. J. Williams. 1995. New insights into the gating mechanisms of cardiac ryanodine receptors revealed by rapid changes in ligand concentration. *Circ. Res.* 77: 765–772.

Smith, J. S., T. Imagawa, J. Ma, M. Fill, K. P. Campbell, and R. Coronado. 1988. Purified ryanodine receptor from rabbit skeletal muscle is the calcium-release channel of sarcoplasmic reticulum. *J. Gen. Physiol.* 92:1–26.

Stern, M. D. 1996. "Adaptive" behavior of ligand-gated ion channels: constraints by thermodynamics. *Biophys. J.* 70:2100–2109.

Swillens, S. 1992. Dynamic control of inositol 1,4,5-trisphosphate-induced Ca^{2+} release: a theoretical explanation for the quantal release of Ca^{2+}. *Mol. Pharmacol.* 41:110–114.

Tang, Y., and H. G. Othmer. 1994. A model of calcium dynamics in cardiac myocytes based on the kinetics of ryanodine-sensitive calcium channels. *Biophys. J.* 67:2223–2235.

Tsugorka, A., E. Rios, and L. A. Blatter. 1995. Imaging elementary events of calcium release in skeletal muscle cells. *Science.* 269:1723–1726.

Vélez, P., X. Li, R. Tsushima, M. Cortes-Gutierrez, A. Wasserstrom, and M. Fill. 1995. Adaptation of single cardiac ryanodine receptor channels may involve a closely associated regulatory protein. *Biophys. J.* 68: A375.

Vélez, P., A. J. Lokuta, H. H. Valdivia, S. Györke, and M. Fill. 1996. Adaptation of cardiac ryanodine receptors. *Biophys. J.* 70:A165.

Wilson, D. L., and A. M. Brown. 1985. Effect of limited interval resolution on single channel measurements with application to Ca channels. *IEEE Trans. Biomed. Eng.* BME-32:786–797.

Yasui, K., P. Palade, and S. Györke. 1994. Negative control mechanism with features of adaptation controls Ca^{2+} release in cardiac myocytes. *Biophys. J.* 67:457–460.

Zahradníková, A., I. Györke, and S. Györke. 1996. Modal transitions during calcium release channel adaptation. *Biophys. J.* 70:A145.

Zahradníková, A., and P. Palade. 1993. Procaine effects on single sarcoplasmic reticulum Ca^{2+} release channels. *Biophys. J.* 64:991–1003.

Zahradníková, A., and I. Zahradník. 1995a. Description of modal gating of the cardiac calcium release channel in planar lipid membranes. *Biophys. J.* 69:1780–1788.

Zahradníková, A., and I. Zahradník. 1995b. The role of modal behavior in the inactivation of cardiac Ca^{2+}-release channels. *Biophys. J.* 68:A374.